Available online at www.sciencedirect.com
ScienceDirect
International Journal of Mass Spectrometry 266 (2007) 50–61
International Journal of Mass Spectrometry
www.elsevier.com/locate/ijms

Charged titanium-doped carbon clusters: Structures and energetics

Laura Largo, Álvaro Cimas, Pilar Redondo, Víctor M. Rayón, Carmen Barrientos *

Departamento de Química Física y Química Inorgánica, Facultad de Ciencias, Universidad de Valladolid, 47005 Valladolid, Spain

Received 1 June 2007; received in revised form 29 June 2007; accepted 29 June 2007
Available online 13 July 2007

Abstract

The structures and stabilities of $TiC_n^{+/-}$ ($n = 1$–8) clusters have been studied by density functional theory (DFT) using the hybrid B3LYP functional. Molecular properties for three different isomers, linear, cyclic and fan species have been computed. The fan isomers, where the titanium atom interacts with the whole carbon chain, are predicted generally, to be more stable than both linear and cyclic structures. For linear and fan $TiC_n^{+/-}$ isomers an even-odd alternation in stability is found, isomers with *n*-even being in general more stable than the adjacent *n*-odd numbered. The ionization potentials and electron affinities of linear and fan TiC_n clusters also show an even–odd parity effect. Generally *n*-odd clusters have higher ionization potentials than the *n*-even ones whereas the electron affinities show an opposite alternation trend, *n*-even systems having higher values than the adjacent *n*-odd ones.

Keywords: Density functional theory; Titanium-doped carbon cluster; Structure and stability

1. Introduction

Carbon clusters have been the subject of extensive theoretical and experimental studies [1–3] because they present important interest in several fields. For example, carbon clusters have attracted attention in Astrophysics, since their detection, a century ago, in astrophysical sources. In addition it is well known that carbon chains are related to the chemistry of carbon stars, comets and interstellar molecular clouds [4–10]. Highly unsaturated hydrocarbons were proposed as potential carriers of some diffuse interstellar bands [11,12]. On the other hand, in gas-phase chemistry, carbon clusters can act as intermediates in chemical vapor deposition systems for the production of silicon carbide films and thin diamond [13,14].

From a structural point of view carbon clusters also deserve attention. These systems may exist in both open-chain and cyclic forms and at a later stage the fullerene cage will dominate [3]. It is well known that carbon chains present important parity effects. For instance, the ground electronic states of linear C_n clusters [15] depend on the parity of the carbon chain and alternate with each new added carbon atom. In particular small pure carbon clusters ($n < 10$) produced by various experimental techniques such as secondary ion mass spectrometry (SIMS), spark source mass spectrometry (SSMS), laser vaporization, or observed in interstellar clouds, show a very markedly parity effect with alternations in the emission intensities of C_n^+ ions (maxima for odd *n*) or C_n^- ions (maxima for even *n*) [16].

Carbon clusters with a heteroatom, XC_n, have also become the focus of recent research interest [17–19] after the discovery of these species in the interstellar medium and in the atmosphere of some planets [20–23]. Some of these systems have been synthesized in the laboratory [24] and they are mostly stable under normal conditions [25].

Similar to pure carbon clusters, heteroatom-doped clusters also present interesting parity effects. These systems are produced from carbides by various experimental techniques, especially SIMS, and show strong alternations in their emission intensities according to the parity of the carbon atom number. It has been shown that this effect can be related to the Pauling electronegativity of the heteroatom [26].

In order to explore these interesting experimental observations, a lot of theoretical investigations on neutral and charged heteroatom-carbon clusters have been carried out. Most of the currently available data for these systems refer to XC_n clusters in which the heteroatom belongs to a first- or second-row element in the periodic table [27–51]. However, the informa-

* Corresponding author. Fax: +34 983 423013.
E-mail address: cbb@qf.uva.es (C. Barrientos).

1387-3806/$ – see front matter © 2007 Elsevier B.V. All rights reserved.
doi:10.1016/j.ijms.2007.06.023

tion about carbon clusters doped with transition metal is scarcer [52–62].

One of the most interesting heteroatoms, from several points of view, in transition-metal doped carbon clusters is titanium. Firstly, from an interstellar chemistry point of view, this element presents a relatively large cosmic abundance [63]; in fact, a binary compound containing titanium, TiO, was identified almost a century ago in cool starts [64]. Even though no metal-containing carbon chain species have been detected in the interstellar or circumstellar media to date, it has been concluded that TiC should be formed in regions of enhanced density in asymptotic giant branch carbon stars [65]. Secondly, from a structural point of view, the interaction between transition metal and carbon is important in understanding different clusters materials, including endohedrofullerenes, catalytic growth of carbon nanotubes, and metallocarbohedrenes (met-cars). Met-cars, containing 8 metal atoms and 12 carbons, were found to form particularly for the early transition metals, Ti_8C_{12} being a prototypical example [66–68]. Despite the intensive research on met-cars the structure and bonding of these unique clusters are still not well understood. Therefore, a systematic understanding of the detailed structure and bonding of the small-metal carbide clusters would lead to valuable insight into the growth and formation of the met-cars [69–77].

The increasing interest in the growth pattern of Ti_8C_{12} has triggered different studies focused on the structure and stabilization energies of small TiC_n clusters. The smallest member in the series, titanium carbide, TiC, has been studied at different levels of theory. Hack et al. [78] carried out an ab initio study of TiC. In their study, a comparison of various ab initio methods, including density functional methods, was made. In particular the results obtained with the hybrid density functional B3LYP were in good agreement with high level ab initio approaches. More recently Kalemos and Mavridis [79] have reported accurate multireference variational calculations on the ground and different excited states of titanium carbide. On the other hand, different neutral and charged TiC_n clusters ($n = 1$–4) have been the subject of several theoretical studies [80–84]. In addition, vibrationally resolved photoelectron spectra were obtained for TiC_n^- ($n = 2$–5) clusters by Wang et al. [85].

Recently, we have carried out a theoretical study of the neutral TiC_n ($n = 1$–8) system [86]. To our knowledge, there exist no theoretical data on $TiC_n^{+/-}$ ($n > 4$) systems, hence the present study complete our previous work on carbon–titanium clusters. We shall focus especially on the structure of the different TiC_n^+ and TiC_n^- ($n = 1$–8) isomers, as well as in the possible regularities that could be observed along the series. The energy calculations of the cationic and anionic species will allow us to estimate some properties as ionization potentials and electron affinities for neutral TiC_n clusters, as well as to discuss their systematic behavior with the size of the cluster. Finally, the competition between the different structures of cationic and anionic systems as a function of the number of carbon atoms will be analyzed.

2. Computational methods

We have employed the same theoretical approach than in our previous study of neutral TiC_n clusters [86].

All calculations were performed using Pople's basis set, 6-311 + G(d) for carbon atoms. This basis set includes diffuse and polarization functions, and is constructed employing the triple split-valence 6-311G(d) [87]. For titanium, we have used the Wachters [88] and Hay [89] basis set, with the scaling factor of Raghavachari and Trucks [90].

The density functional theory (DFT), in particular the B3LYP exchange-correlation functional [91,92] was used throughout. The acronym stands for Lee et al. [92] correlation functional in conjunction with Becke's hybrid exchange functional [93].

Energetics are addressed at the B3LYP/6-311 + G(d) level. Previous studies have shown that this level provides results for medium-sized heteroatom-doped carbon clusters in good agreement with experimental results [94].

All these calculations were carried out with the *Gaussian-98* program package [95].

3. Results and discussion

We have carried out a study of the charged $TiC_n^{+/-}$ ($n = 1$–8) isomers, on the doublet and quartet potential energy surfaces. It must be pointed out that in general sextuplet states are not competitive because they lie higher in energy with the exception of linear TiC_n^- clusters. Thus, for these systems we have also included results for the sextuplet potential energy surface. In particular, we have found three conformations on each potential energy surface: (a) linear structures with the titanium atom sited at the end position; (b) cyclic structures, where titanium is bonded essentially to the two terminal carbon atoms of the C_n unit; (c) "fan" structures, where titanium interacts with the whole carbon chain.

In order to analyze systematic trends in the different properties considered, we will discuss the data for each type of structure separately giving results for some properties considered as the electronic energies and dipole moments. Other molecular properties which might be helpful in possible experimental studies, vibrational frequencies or rotational constants, are provided as Supporting Information (Tables S1–S6).

3.1. Structure and molecular properties of TiC_n^+ clusters

The results for linear TiC_n^+ clusters, namely total energies (electronic plus zero point vibrational energy, ZPE), S^2 expectation values, binding energies, dipole moments and relative energies at the B3LYP/6-311 + G(d) level are listed in Table 1. The corresponding geometries of the predicted lowest-lying species are shown in Fig. 1. All reported linear structures are true minima on their respective potential energy surface, since all of them have real vibrational frequencies (see Table S1).

From Table 1 it can be seen that the ground state of linear TiC_n^+ clusters alternates between $^2\Delta$ (even n) and $^4\Delta$ (odd n), except the first member in the series (TiC^+, $^2\Sigma^+$). These lowest-lying states can be related to their electronic configuration. TiC_n^+

Table 1
Electronic energies (including ZPE correction), $\langle S^2 \rangle$ values, binding energies, dipole moments, and relative energies, for linear TiC_n^+ clusters at the B3LYP/6-311 + G(d) level

Isomer	State	$-E$ (au)	$\langle S^2 \rangle$	BE (eV)	μ (D)	ΔE (kcal mol^{-1})
TiC^+	$^2\Sigma^+$	887.093607	0.764	3.45	4.70	0.00
	$^4\Phi$	887.072967	3.756	2.88	4.50	12.95
TiC_2^+	$^2\Delta$	925.191109	0.852	9.98	8.67	0.00
	$^4\Sigma^-$	925.156336	3.811	9.04	6.83	21.82
TiC_3^+	$^2\Pi$	963.243785	1.076	15.30	10.79	18.79
	$^4\Delta$	963.273737	3.786	16.11	9.52	0.00
TiC_4^+	$^2\Delta$	1001.364037	1.209	22.46	12.45	0.00
	$^4\Delta$	1001.337083	3.778	21.72	13.22	16.91
TiC_5^+	$^2\Pi$	1039.419938	1.272	27.86	15.15	18.98
	$^4\Delta$	1039.450191	3.822	28.69	13.03	0.00
TiC_6^+	$^2\Delta$	1077.536365	1.450	34.91	15.94	0.00
	$^4\Sigma^-$	1077.521299	3.812	34.50	16.74	9.45
TiC_7^+	$^2\Delta$	1115.610419	1.804	40.81	17.86	7.81
	$^4\Delta$	1115.623123	3.861	41.16	16.42	0.00
TiC_8^+	$^2\Delta$	1153.707694	1.634	47.34	19.28	0.00
	$^4\Pi$	1153.669154	3.790	46.30	22.95	24.18

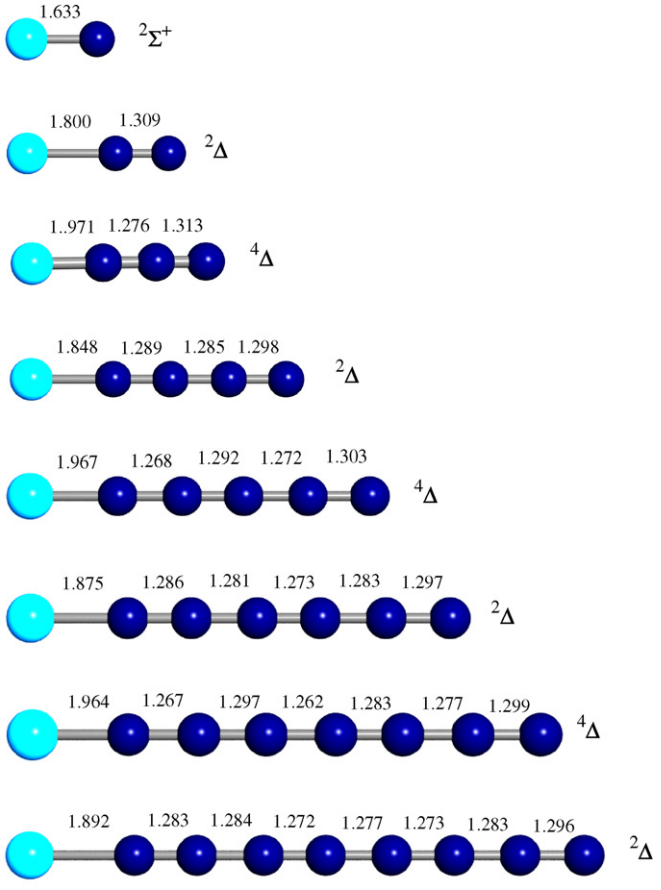

Fig. 1. Optimized geometries of linear TiC_n^+ isomers at the B3LYP/6-311 + G(d) level. Distances are in angstroms.

clusters have $4n + 3$ (n being the number of carbon atoms in the cluster) valence electrons which are distributed over the valence orbitals as follows:

$$\{\text{core}\}1\sigma^2 \ldots 1\pi^4 \ldots (n+1)\sigma^2 \left(\frac{n}{2}\right) \pi^4 1\delta^1 \quad n\text{-even clusters}$$

$$\{\text{core}\}1\sigma^2 \ldots 1\pi^4 \ldots (n+1)\sigma^2 \left(\frac{n+1}{2}\right) \pi^2 1\delta^1 \quad n\text{-odd clusters}$$

except for TiC^+ ($^2\Sigma^+$: $\{\text{core}\}1\sigma^2 1\pi^4 2\sigma^1$).

Thus cationic TiC_n^+ clusters are obtained by removing a σ electron from frontier $(n+2)\sigma$ orbital of neutral TiC_n [86].

Cationic TiC_n^+ clusters contain $2n+2$ valence σ-electrons, $2n$ valence π-electrons and a valence δ-electron. The valence σ-electrons fully occupy $n+1$ σ-orbitals. When n is even, the $2n$ π-electrons fully occupy $n/2$ π-orbitals and the resulting configurations $\sigma^2\pi^4\delta^1$ lead to $^2\Delta$ states. For the species with odd n, however, two of the $2n$ π-electrons are distributed over a half-filled π-orbital, so that the lowest energy states are $^4\Delta$.

According to the bond lengths given in Fig. 1, two types of behaviors can be distinguished. For even n clusters, C–C bond lengths tend to average out (in the range 1.272–1.299 Å) along the straight C_n chains, the last C–C bond of the C_n chain being the longest one. Consequently n even TiC_n^+ clusters show some degree of cumulene character. For n odd species, there is a weak alternating short and long pattern in C–C lengths (C_{odd}–C_{even} distances being slightly shorter than C_{even}–C_{odd} ones) reflecting some sort of polyacetylene character.

The Ti–C bond distances show a short/long alternation with even/odd n. Thus, for even n the bond lengths are within 1.800–1.892 Å, and we can observe a slight increase with increasing number of carbon atoms. On the other hand, for n odd clusters (except TiC^+) bond distances are in the range 1.964–1.971 Å and slightly decrease with increasing n. In addition the Mulliken population analyses show that the positive charge is located at the titanium atom (as an example, the net charges are +1.11 and +1.13 for TiC_4^+ and TiC_6^+, respectively). In n-even clusters, the unpaired electron is located at the titanium atom. Consequently, the dominant valence structures contributing to the description of n-even TiC_n^+ clusters could be depicted as:

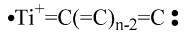

whereas in n-odd species the unpaired electrons are distributed between titanium and the terminal carbon atom, and the valence structures are intermediate between:

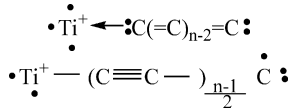

There are two previous studies of the first member of the series, TiC^+. Kerkines and Mavridis [84] carried out a complete study on the ground and low-lying states of titanium carbide cation using multireference methods coupled with quantitative basis sets. In their work, they constructed potential energy curves for the ground and twelve low-lying excited states for TiC^+ and predicted a ground state of $^2\Sigma^+$ symmetry with the first excited state, $^2\Pi$, located 14.6 kcal/mol above

the ground state. They also found two practically degenerated states, $^4\Pi$ and $^4\Phi$, located 17.7 and 17.8 kcal/mol (at the MRCI level), respectively, above the ground state. Their MRCI (MCRI + Davidson correction) binding energy was estimated to be $D_0 = 85.2$ (86.7) kcal/mol in good agreement with the experimental data of 93.39 ± 5.53 kcal/mol [96]. On the other hand, Gutsev et al. [97] carried out a systematic study of the structure and properties of different charged and neutral XC (X being a 3d-metal) systems using density functional theory (DFT) and hybrid DFT methods.

Our calculations predict a $^2\Sigma^+$ ground state with a $^4\Phi$ state lying about 13 kcal/mol higher in energy. We obtain a binding energy, $D_0 = D_e - (\omega_e)/2$, for $^2\Sigma^+$ of 79.33 kcal/mol, and a Ti–C distance of 1.633 Å, not too far from the MRCI (1.696 Å) and MRCI + Q (1.70 Å) values [84]. Obviously, there is a rather close agreement between our results for monocarbide cation and those computed by Gutsev et al. [97].

The ground state of the titanium-carbide cation results from interaction of the ground state of the titanium cation $Ti^+(^4F, 4s^1 3d^2)$ and the ground state of carbon $C(^3P, 2s^2 2p^2)$. Thus, two covalent π bonds can be formed, and in addition the bonding may be enhanced by donation of the nonbonding $3d_\sigma$ electron of Ti^+ into the empty p_σ orbital on the carbon atom. Then the overall bond order for TiC^+ is approximately 2(1/2) (two π bonds and a half σ bond) [84]. This ground state could be represented by the following valence bond picture: $^+Ti \overline{\overline{\cdots\bullet\cdots}} C:$

It is also interesting to compare the predicted vibrational frequency with the available theoretical result. We have obtained a value of 984 cm^{-1} for the Ti–C stretching mode in reasonable agreement with that reported by Kerkines and Mavridis [84] of 859 cm^{-1} (MRCI level of theory).

Table 2
Electronic energies (including ZPE correction), $\langle S^2 \rangle$ values, binding energies, dipole moments, and relative energies for cyclic TiC_n^+ clusters at the B3LYP/6-311 + G(d) level

Isomer	State	$-E$ (au)	$\langle S^2 \rangle$	BE (eV)	μ (D)	ΔE (kcal mol^{-1})
TiC_2^+	$^2A_2$	925.219849	0.791	10.77	6.05	0.00
	$^4A''$	925.189192	3.768	9.93	5.90	19.24
TiC_3^+	$^2A_2$	963.284373	1.171	16.41	7.30	0.00
	$^4B_2$	963.280723	3.761	16.31	6.11	2.29
TiC_5^+	$^2B_1$	1039.425340	0.765	28.01	6.16	
TiC_6^+	$^2A''$	1077.541944	0.798	35.07	6.39	0.00
	$^4A''$	1077.506726	3.776	34.11	5.08	22.10
TiC_7^+	$^2A_2$	1115.622408	0.776	41.14	5.09	1.53
	$^4A_1$	1115.624849	3.857	41.21	4.17	0.00
TiC_8^+	$^2B_1$	1153.735369	0.775	48.10	3.37	0.00
	$^4A''$	1153.685139	3.780	46.73	0.30	31.52

Data for the cyclic TiC_n^+ clusters are provided in Table 2 and the geometries for the corresponding lowest-lying species are displayed in Fig. 2. It must be noted that for some clusters (TiC_4^+ and quartet TiC_5^+) we do not report data, since all our attempts to obtain cyclic structures for these species collapsed into the corresponding fan structures.

From Table 2 we can see that in general doublet states are favored over quartet ones, with the exception of TiC_7^+ where a quartet ground state is predicted, although the doublet state is just 1.53 kcal/mol higher in energy and both structures have been

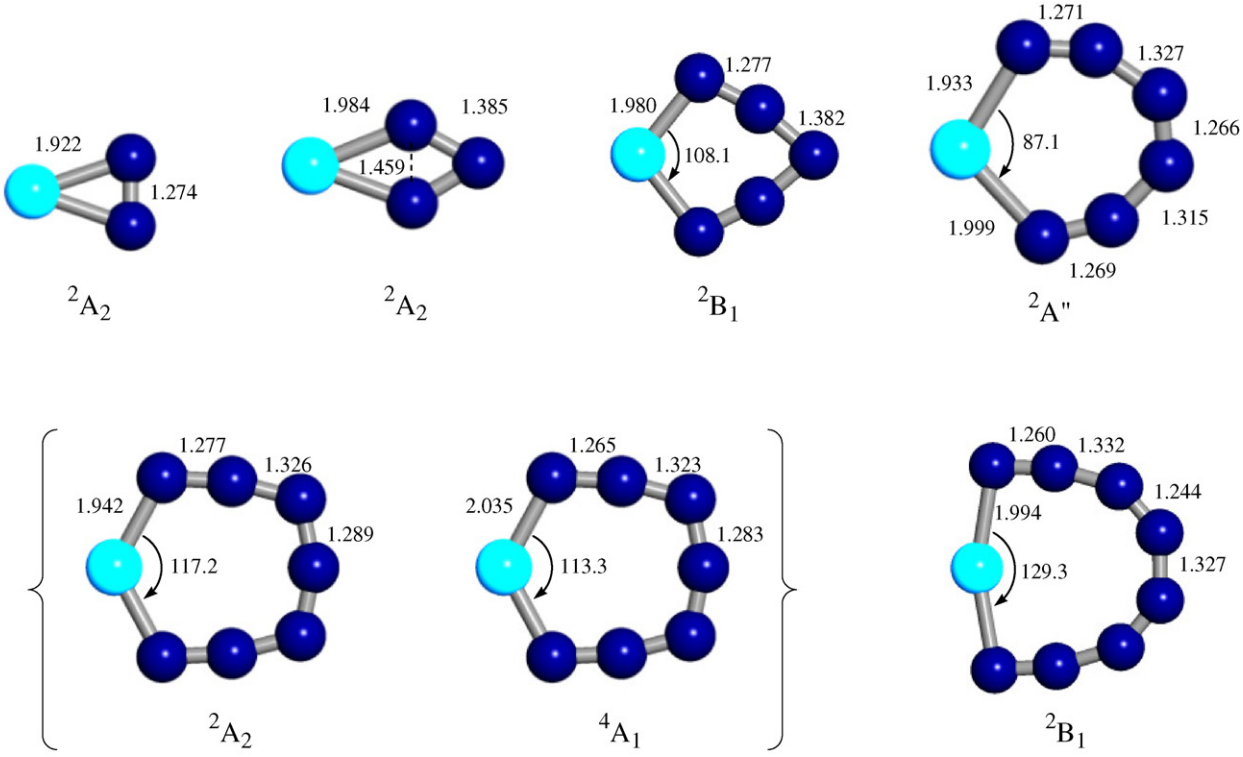

Fig. 2. Optimized geometries of cyclic TiC_n^+ isomers at the B3LYP/6-311 + G(d) level. Distances are in angstroms and angles in degrees.

included in Fig. 2. As it can be seen from Table 2, the quartet-doublet energy difference is greater for *n*-even clusters than in the case of *n*-odd ones. The dipole moments, also shown in Table 2, are relatively high but decrease significantly for TiC_8^+.

It can be observed from Fig. 2 a clear alternation in C–C bond distances, in general C_{odd}–C_{even} distances being shorter than C_{even}–C_{odd} ones, following a similar pattern than that observed for *n*-even linear TiC_n^+ clusters.

The molecular properties, namely, absolute, binding and relative energies, S^2 expectation values and dipole moments for the low-lying doublet and quartet states of fan-type TiC_n^+ clusters are reported in Table 3. In Fig. 3, the geometries of the ground states of fan TiC_n^+ species are displayed.

All the structures showed in Table 3 are true minima on their corresponding potential energy surfaces (see Table S3).

It is readily seen in Table 3 that all fan TiC_n^+ clusters present doublet ground states. However, in the case of TiC_7^+ our B3LYP results show that both states, doublet and quartet, are virtually isoenergetic (differing by just 0.23 kcal/mol), consequently both structures are shown in Fig. 3. For the quartet state of TiC_8^+ we only found the cyclic structure, all our attempts to find the fan arrangement led to the cyclic conformation. In *n*-even fan TiC_n^+ clusters quartet states are not competitive, since they lie considerably higher in energy.

The Ti–C bond distances for fan structures are, in general, longer than in both linear and cyclic conformations. In fan clusters there exists a π-type interaction between the titanium and the entire C_n unit; consequently all the Ti–C distances are very close. In some cases the distances between titanium atom and a non-terminal carbon are even slightly shorter than the corresponding distances between Ti and the terminal carbon atoms. As a consequence of the interaction with the entire carbon unit, for the largest species, TiC_7^+ and TiC_8^+, the titanium atom is almost *embedded* in the carbon chain. On the other hand, we found the same alternation in C–C distances for fan clusters than

Table 3
Electronic energies (including ZPE correction), $\langle S^2 \rangle$ values, binding energies, dipole moments, and relative energies for fan TiC_n^+ clusters at the B3LYP/6-311 + G(d) level

Isomer	State	$-E$ (au)	$\langle S^2 \rangle$	BE (eV)	μ (D)	ΔE (kcal mol^{-1})
TiC_3^+	$^2A_2$	963.285174	0.757	16.43	5.59	0.00
	$^4B_1$	963.275215	3.800	16.16	5.11	6.25
TiC_4^+	$^2A_1$	1001.399120	0.759	23.41	3.90	0.00
	$^4A_2$	1001.339874	3.778	21.80	4.45	37.18
TiC_5^+	$^2B_1$	1039.447797	0.777	28.62	2.27	0.00
	$^4A'$	1039.439154	3.824	28.39	3.08	5.40
TiC_6^+	$^2A_1$	1077.547227	0.758	35.21	0.14	0.00
	$^4A''$	1077.499964	3.803	33.92	1.30	29.66
TiC_7^+	$^2A'$	1115.602766	0.764	40.60	2.58	0.23
	$^4B_1$	1115.603136	3.854	40.61	1.53	0.00
TiC_8^+	$^2A'$	1153.703197	0.757	47.22	3.50	0.00
	$^4A'$	1153.647941	3.795	45.72	2.58	34.67

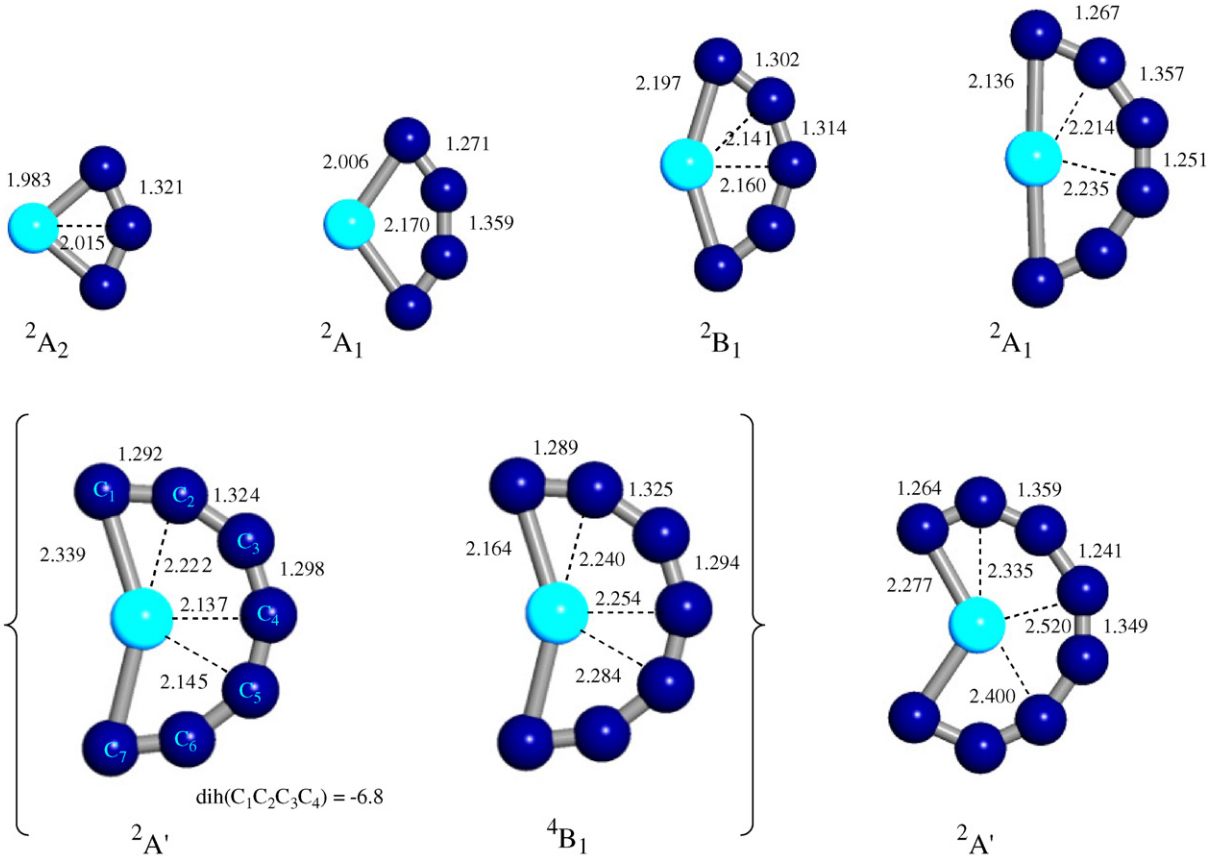

Fig. 3. Optimized geometries of fan TiC_n^+ isomers at the B3LYP/6-311 + G(d) level. Distances are in angstroms and angles in degrees.

Table 4
Electronic energies (including ZPE correction), $\langle S^2 \rangle$ values, binding energies, dipole moments and relative energies for linear TiC_n^- clusters at the B3LYP/6-311 + G(d) level

Isomer	State	$-E$ (au)	$\langle S^2 \rangle$	B (eV)	μ (D)	ΔE (kcal mol^{-1})
TiC^-	$^2\Sigma^+$	887.388088	0.754	4.38	1.71	0.00
	$^4\Phi$	887.371175	3.780	3.92	3.03	10.61
	$^6\Phi$	887.339480	8.813	3.05	0.75	30.50
TiC_2^-	$^2\Delta$	925.539841	1.006	12.39	4.38	0.00
	$^4\Delta$	925.535284	3.761	12.27	7.69	2.86
	$^6A'$	925.457433	8.762	1.15	0.66	51.71
TiC_3^-	$^2\Pi$	963.586888	1.616	17.55	6.30	2.95
	$^4\Phi$	963.591593	4.188	17.68	8.14	0.00
	$^6A''$	963.583614	8.778	17.47	6.54	5.01
TiC_4^-	$^2\Delta$	1001.722906	1.115	25.14	7.44	0.00
	$^4\Phi$	1001.722126	3.768	25.12	11.54	0.49
	$^6\Phi$	1001.658681	8.763	23.39	4.69	40.30
TiC_5^-	$^2\Pi$	1039.769272	1.107	30.29	6.70	10.15
	$^4\Phi$	1039.785446	4.289	30.73	11.31	0.00
	$^6\Phi$	1039.777692	8.800	30.51	10.53	4.87
TiC_6^-	$^2\Delta$	1077.898691	1.153	37.69	10.25	2.88
	$^4\Phi$	1077.903276	3.770	37.82	15.32	0.00
	$^6\Phi$	1077.847683	8.773	36.30	7.90	34.88
TiC_7^-	$^2\Pi$	1115.945415	0.789	42.85	10.18	14.62
	$^4\Phi$	1115.968712	4.355	43.48	14.36	0.00
	$^6\Phi$	1115.963032	8.821	43.33	14.04	3.56
TiC_8^-	$^2\Delta$	1154.022032	0.761	48.82	19.82	39.19
	$^4\Phi$	1154.084482	3.770	50.51	18.58	0.00
	$^6\Phi$	1154.033393	8.787	49.12	11.17	32.06

in the linear and cyclic species, C_{odd}–C_{even} distances shorter than C_{even}–C_{odd}, especially in n-even clusters.

3.2. Structure and molecular properties of TiC_n^- clusters

The molecular properties, absolute, relative and binding energies, S^2 expectation values and dipole moments for the lowest-lying doublet and quartet states for linear TiC_n^- clusters are given in Table 4, and the geometries of the ground states of TiC_n^- species are shown in Fig. 4. We must point out that for linear TiC_n^- systems we have included results for sextuplet states because they are located very close in energy to the corresponding ground states, especially in the case of n odd clusters.

All the linear structures reported in Fig. 4 are true minima on their respective potential energy surface (see Table S4). It is readily seen in Table 4 that linear TiC_n^- clusters present $^4\Phi$ ground states, excepting the two first members in the series. In n-odd linear TiC_n^- clusters the first excited state corresponds in general to a $^6\Phi$ symmetry and the sextuplet-quartet energy differences slightly decreases along the series being just 3.56 kcal/mol for $n = 7$. In n-even TiC_n^- clusters the first excited states are mainly of $^2\Delta$ symmetry, and in the case of TiC_4^- our results show that both doublet and quartet states are virtually isoenergetic. As we mentioned in linear TiC_n^+ clusters the stability of the different states will be explained in terms of their electronic configuration. TiC_n^- clusters present $4n + 5$ valence electrons, and

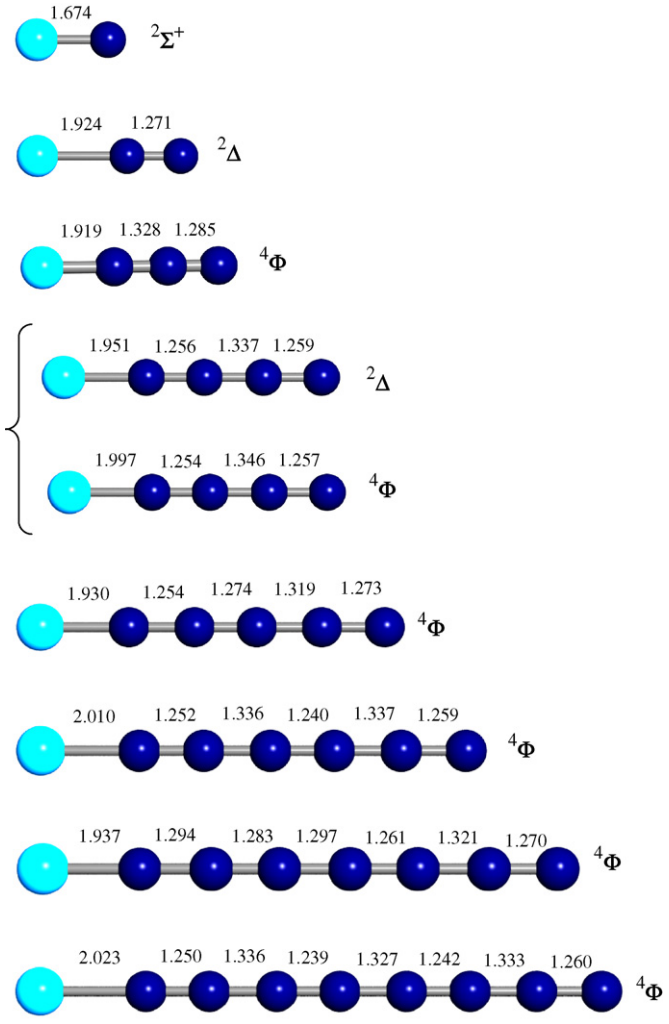

Fig. 4. Optimized geometries of linear TiC_n^- isomers at the B3LYP/6-311 + G(d) level. Distances are in angstroms.

in $^4\Phi$ states the corresponding electronic configuration can be depicted as:

$$\{\text{core}\}1\sigma^2 \ldots 1\pi^4 \ldots (n+1)\sigma^2(n+2)\sigma^1 \left(\frac{n+1}{2}\right) \pi^3 1\delta^1$$

n-odd clusters

$$\{\text{core}\}\, 1\sigma^2 \ldots 1\pi^4 \ldots (n+1)\, \sigma^2\, (n+2)\, \sigma^1 \left(\frac{n+2}{2}\right) \pi^1 1\delta^1$$

n-even clusters

except for TiC^- ($^2\Sigma^+$: $\{\text{core}\}1\sigma^2 2\sigma^2 1\pi^4 3\sigma^1$) and TiC_2^- ($^2\Delta$:$\{\text{core}\}1\sigma^2 2\sigma^2 1\pi^4 3\sigma^2 4\sigma^2 1\delta^1$).

Consequently, anionic clusters are obtained by adding an electron to frontier π orbital of neutral TiC_n [86].

In the case of n-odd TiC_n^- clusters the lowest-lying $^6\Phi$ state can be obtained upon a $[(n+1)/2]\pi \rightarrow [(n+3)/2]\pi$ promotion. Both orbitals are mainly located at the titanium atom and the energy difference between the resulting configuration $\sigma^1\pi^2\delta^1\pi^1$ and the ground state one $\sigma^1\pi^3\delta^1$ is really small.

There is only one available theoretical result for the first member of the series TiC^-. Gutsev et al. [97] found a $^2\Sigma^+$ ground state in good agreement with our results for this species.

From Fig. 4, it can be seen that the straight C_n chains of TiC_n^- clusters show in general cumulene-like character:

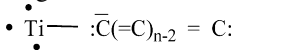

However in the case of *n*-even linear TiC_n^- clusters the carbon–carbon distances indicate certain polyacetylenic character. Consequently in these clusters the valence bond picture will be intermediate between the cumulene-like scheme and the following one:

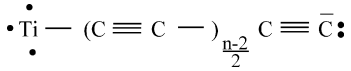

The dipole moments of linear TiC_n^- clusters are in all cases high and increase with the number of carbon atoms.

The different molecular properties studied in this work corresponding to cyclic and fan anionic isomers are given in Tables 5 and 6, respectively. The corresponding vibrational frequencies and rotational constants are provided as Supplementary Material in Tables S5 (cyclic TiC_n^- isomers) and S6 (fan TiC_n^- clusters). As can be seen from Tables S5 and S6, all reported cyclic and fan structures for the anionic clusters are true minima on their respective potential energy surface.

Table 5
Electronic energies (including ZPE correction), $\langle S^2\rangle$ values, binding energies, dipole moments and relative energies for cyclic TiC_n^- clusters at the B3LYP/6-311 + G(d) level

Isomer	State	$-E$ (au)	$\langle S^2\rangle$	BE (eV)	μ (D)	ΔE (kcal mol^{-1})
TiC_2^-	$^2A_2$	925.539248	1.469	12.37	0.96	7.28
	$^4B_1$	925.550845	3.758	12.69	2.91	0.00
TiC_3^-	$^4B_2$	963.605053	3.763	18.05	2.97	
TiC_5^-	$^4B_2$	1039.777731	3.766	30.52	2.99	
TiC_6^-	$^2A'$	1077.863911	1.524	36.74	6.82	19.81
	$^4A''$	1077.895477	3.770	37.60	3.17	0.00
TiC_7^-	$^2B_1$	1115.991410	0.833	44.10	5.95	3.65
	$^4B_2$	1115.997228	3.780	44.26	2.37	0.00
TiC_8^-	$^2A'$	1154.091369	0.771	50.70	2.23	0.00
	$^4B_1$	1154.076609	3.772	50.30	2.08	9.26

From Table 5, we can conclude that, except for TiC_8^-, cyclic TiC_n^- clusters present quartet ground states. However it should be noted that we have not found doublet states for TiC_3^- and TiC_5^- clusters because they evolved towards the corresponding fan structures. In the case of fan structures (Table 6), we can see that doublet states are favored over quartet states. However for $n = 8$ both doublet and quartet are practically isoenergetic.

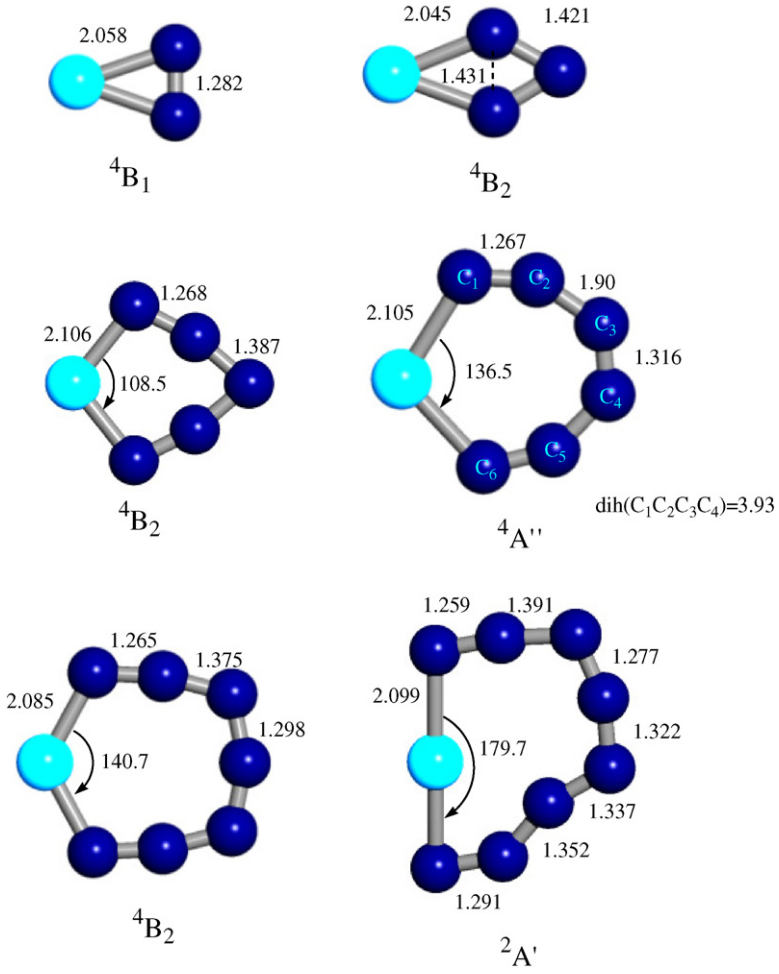

Fig. 5. Optimized geometries of cyclic TiC_n^- isomers at the B3LYP/6-311 + G(d) level. Distances are in angstroms and angles in degrees.

Table 6
Electronic energies (including ZPE correction), $\langle S^2 \rangle$ values, binding energies, dipole moments and relative energies for fan TiC_n^- clusters at the B3LYP/6-311 + G(d) level

Isomer	State	$-E$ (au)	$\langle S^2 \rangle$	BE (eV)	μ (D)	ΔE (kcal mol^{-1})
TiC_3^-	$^2A_2$	963.631973	0.764	18.78	1.48	0.00
	$^4A_2$	963.614923	3.772	18.32	0.45	10.70
TiC_4^-	$^2A_1$	1001.772321	1.588	26.48	0.85	0.00
	$^4B_1$	1001.738681	3.764	25.57	1.36	21.11
TiC_5^-	$^2A'$	1039.826990	0.763	31.86	2.05	0.00
	$^4A_1$	1039.814033	3.779	31.50	1.31	8.13
TiC_6^-	$^2A_1$	1077.914296	0.769	38.12	0.62	0.00
	$^4A_2$	1077.905802	3.769	37.88	0.96	5.33
TiC_7^-	^2A	1116.011140	0.758	44.64	2.56	0.00
	$^4B_2$	1115.987344	3.781	43.99	2.52	14.93
TiC_8^-	$^2B_1$	1154.071272	1.790	50.16	3.12	0.42
	$^4A''$	1154.071937	3.777	50.17	3.18	0.00

As expected, dipole moments for cyclic and fan structures are always lower than those found for linear isomers.

In Figs. 5 and 6, the geometries for the ground states of cyclic and fan anionic clusters are shown. In general, the Ti–C distances are larger for fan structures than for the corresponding cyclic ones and in both structures these distances are larger than those in linear TiC_n^- species. Concerning the C–C bond distance, we observe a behavior quite similar to that found for cationic cyclic and fan clusters: an alternation of C–C bond distances, C_{odd}–C_{even} bond distances being shorter than C_{even}–C_{odd} ones.

3.3. Stability of $TiC_n^{+/-}$ clusters

As in previous works in heteroatom-doped carbon clusters we will employ the concept of incremental binding energy [2,39] to discuss the relative stability of the $TiC_n^{+/-}$ clusters with different sizes. The relative stability of $TiC_n^{+/-}$ clusters can be estimated by computing the consecutive binding energy differences between adjacent $TiC_n^{+/-}$ and $TiC_{n-1}^{+/-}$ clusters. In order to obtain meaningful results we must compare clusters of different size but corresponding to the same type of isomers. For example, incremental binding energies for linear TiC_n^+ clusters can be computed from the values shown in Table 1 as the consecutive binding energy differences between adjacent TiC_n^+ and TiC_{n-1}^+ clusters taken in each case the lowest-lying state. The same procedure employing the values in Tables 2 and 3 provides incremental binding energies for cyclic and fan TiC_n^+ isomers, respectively.

In Fig. 7a the incremental binding energies for the three types of TiC_n^+ clusters, namely, linear, cyclic and fan, are displayed as a function of the number of carbon atoms.

From Fig. 7a we can observe a slight odd–even alternation in stability for linear TiC_n^+ clusters especially in the first members in the series, with even n members being slightly more stable than those with odd $n-1$ and $n+1$ carbon atoms. How-

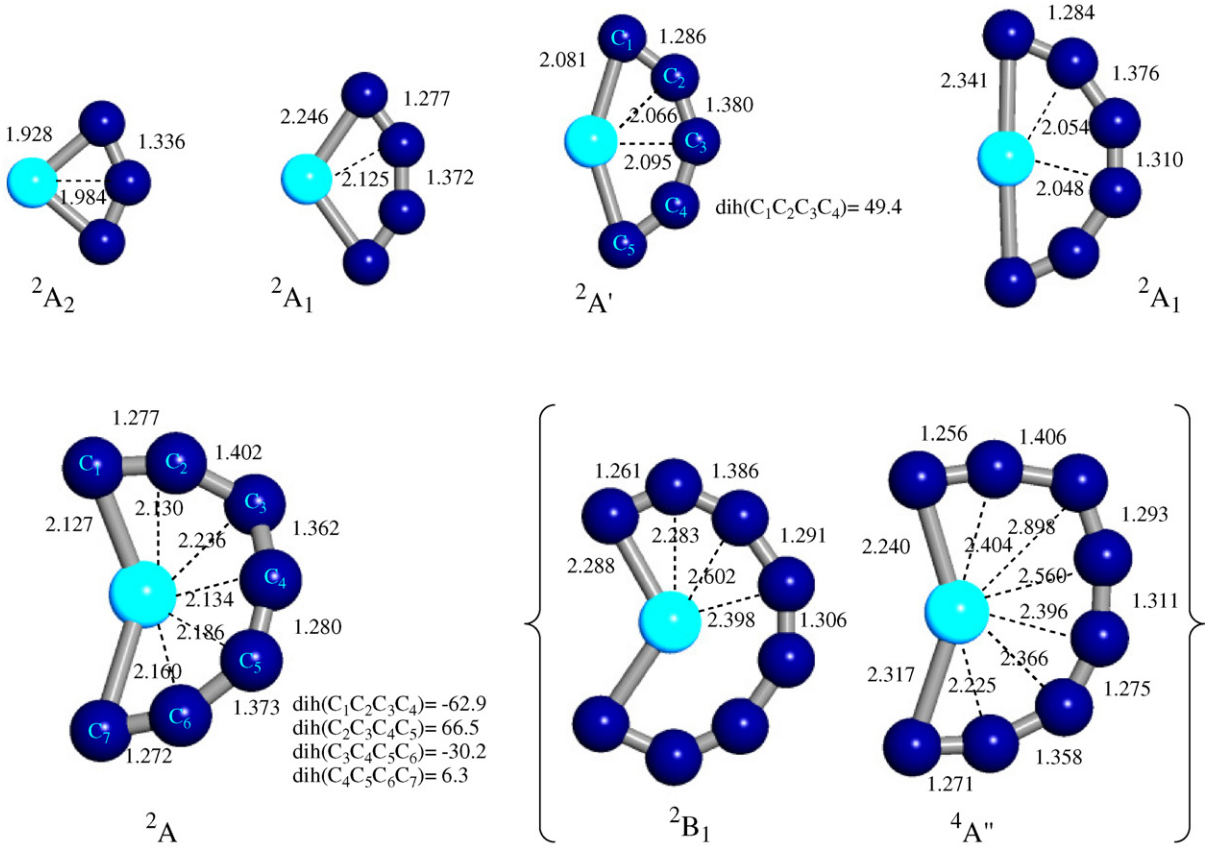

Fig. 6. Optimized geometries of fan TiC_n^- isomers at the B3LYP/6-311 + G(d) level. Distances are in angstroms and angles in degrees.

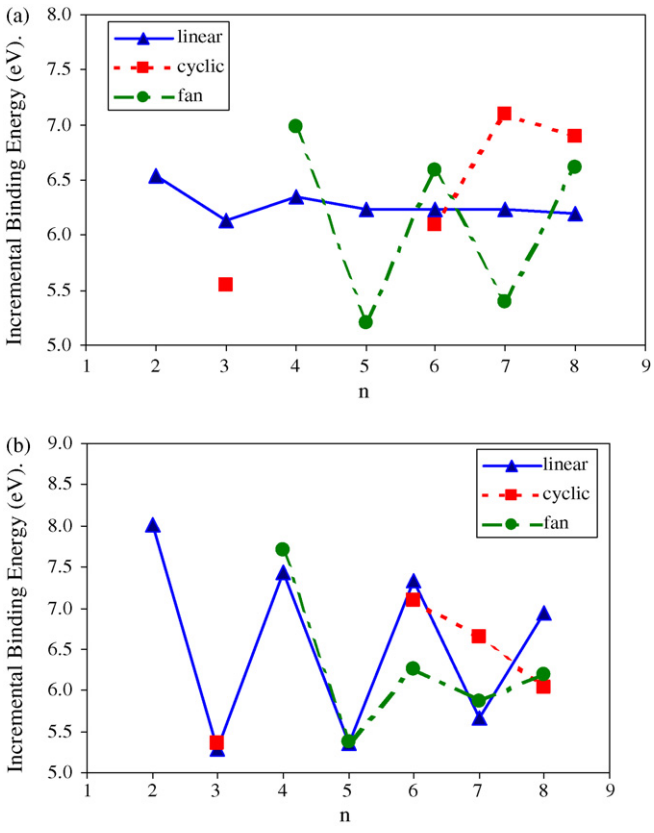

Fig. 7. Incremental binding energies (eV) for the different isomers vs. the number of carbon atoms. (a) TiC_n^+ clusters; (b) TiC_n^- clusters.

ever the last members do not show this pattern. This difference in stability between *n*-odd and *n*-even clusters can be attributed to the electron number in π-type and δ-type highest occupied molecular orbitals. A ground state corresponding to a $\pi^4\delta^1$ electronic configuration (*n*-even) is energetically more favorable than a $\pi^2\delta^1$ one corresponding to *n*-odd clusters. In the case of fan clusters, the incremental binding energies follow the same general pattern as their linear analogues. Clusters with even *n* appear more stable than those with odd *n* and the differences in stability are larger than in the linear clusters. For cyclic isomers, incremental binding energies can only be computed for some members in the series, and therefore we cannot extract any conclusions about the parity effect in the stability of these clusters.

The variation of the incremental binding energy for the different linear, cyclic and fan TiC_n^- clusters versus the number of carbon atoms is displayed in Fig. 7b. For linear isomers, we observe a clear even–odd alternation in stability; *n*-even clusters are more stables than the adjacent *n*-odd ones. In the case of fan structures we also found a clear even–odd alternation in the incremental binding energy, again clusters with an even number of carbon atoms being more stables than the adjacent *n*-odd numbered. However, it can be seen that the difference in stability between *n*-odd and *n*-even in both cases, linear and fan structures, is attenuated as the number of carbon atoms increases, suggesting that the incremental binding energy converges to an almost constant value for larger clusters. In fact the incremental binding energy for the largest species closely approaches a value of nearly 6 eV. Similar to cyclic cationic clusters, it is difficult to find a general trend in the incremental binding energies of cyclic anionic clusters because the lack of data for these species, but we can see, in both cationic and anionic clusters, a stabilization with the size of the clusters.

The relative energies of the different linear and cyclic $TiC_n^{+/-}$ clusters as a function of the number of carbon atoms are shown in Fig. 8 (Fig. 8a contains data for TiC_n^+ clusters and Fig. 8b includes results for TiC_n^- clusters). These relative energies were computed taking as reference the energy of the fan isomers, thus a negative value means that the linear or cyclic structure is more stable than the corresponding fan one. From Fig. 8a we can see that for the TiC_n^+ clusters, in general, the lowest-lying species are the fan isomers, except for $n = 5, 7, 8$. In TiC_5^+ systems the linear conformation is slightly more stable. For $n = 7$ linear and cyclic isomers are practically isoenergetic and both structures are more stable than the corresponding fan one and for $n = 8$ the cyclic specie appears as the global minimum. In the case of anionic clusters, we observe that in all cases the lowest-lying species correspond to fan structures, except for $n = 8$ where a cyclic structure is preferred. In general, it seems that linear and especially cyclic structures are preferred for larger clusters in both cationic and anionic systems.

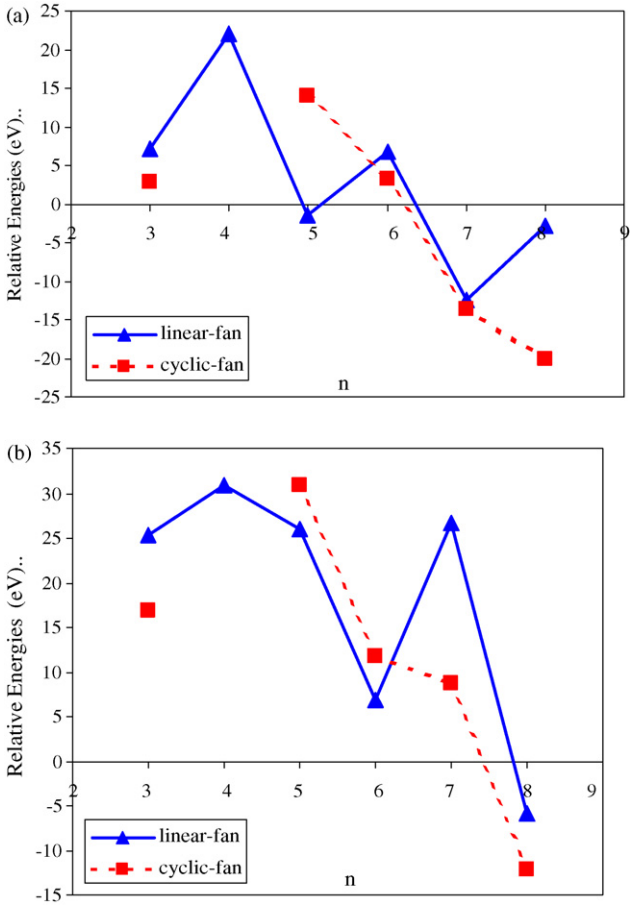

Fig. 8. Relative energies (kcal/mol) of the linear and cyclic isomers with respect to the corresponding fan structures vs. the number of carbon atoms. (a) TiC_n^+ clusters; (b) TiC_n^- clusters.

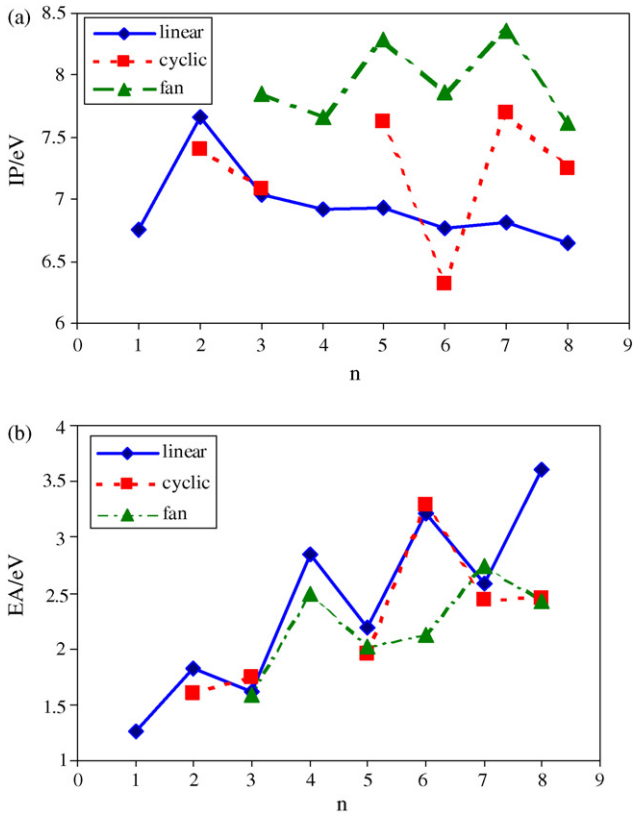

Fig. 9. Ionization potential (IP) and electron affinity (EA), in eV, of linear, cyclic and fan TiC_n clusters vs. the number of carbon atoms. (a) Ionization potential; (b) electron affinity.

3.4. Ionization potential and electron affinity of TiC_n clusters

The ionization potential (IP) and electron affinity (EA) for the TiC_n species as a function of the size of the cluster are shown in Fig. 9 (in Fig. 9a the ionization potentials are collected whereas the electron affinities are displayed in Fig. 9b). We have computed the ionization potentials and electron affinities in their adiabatic version, employing the optimized geometry for the corresponding charged and neutral species.

From Fig. 9a it can be observed that linear TiC_n clusters present a clear even–odd alternation in the IP for the first members in the series, *n*-even members present higher IP than the adjacent *n*-odd ones, however, when *n* increases just a slight even–odd parity effect is found (*n*-odd clusters having higher IPs than the *n*-even ones). In the fan and cyclic structures, the IPs exhibit a clear parity effect, with *n*-odd structures having higher values of the IP than the adjacent *n*-even ones. These behaviors can be related to the stability of linear, cyclic and fan structures of TiC_n/TiC_n^+ clusters. The alternation in the incremental binding energies of linear TiC_n^+ clusters is similar to that found in TiC_n species [86] (*n*-even linear TiC_n/TiC_n^+ being more stable than *n*-odd ones). This leads to a smooth variation in the linear ionization potentials. It can also be observed that for the last members in the series the ionization potential for linear TiC_n show slight variations. This trend arises from the fact that TiC_n^+ clusters can be obtained from the detachment of one electron located at the titanium atom, and consequently the ionization potentials of TiC_n clusters are quite similar to that found for titanium (6.83 eV). In the case of fan and cyclic structures the variation in the incremental binding energy for the TiC_n clusters is opposite to that found in the corresponding TiC_n^+ clusters, this results in a clear even–odd alternation in the IPs.

Finally, concerning the adiabatic electron affinities shown in Fig. 9b, we observe a clear parity effect in the electron affinities of linear TiC_n clusters. Again this tendency is related to the stability of TiC_n and TiC_n^- clusters. The electron affinities for C_n clusters [3] alternate between large values for *n*-even and small for *n*-odd. TiC_n^- clusters can be obtained from attachment of an electron to TiC_n clusters mainly to the C_n unit. Therefore electron affinities of TiC_n clusters will be similar to that of C_n clusters, and the effect of the titanium atom is a slight stabilization of neutral clusters respect to anionic ones.

4. Conclusions

We have performed a DFT study of $TiC_n^{+/-}$ clusters at the B3LYP/6-311 + G(d) level. Three different structures, namely linear, cyclic, and fan structures in their doublet and quartet energy surfaces were considered.

We have provided predictions for different molecular properties such as geometrical parameters, dipole moments, vibrational frequencies and rotational constants that could be useful for a possible experimental study.

For linear TiC_n^+ clusters we have found an alternation in stability between doublet and quartet states, *n*-even TiC_n^+ clusters present $^2\Delta$ ground states whereas *n*-odd numbered have $^4\Delta$ ones, excepting the first member in the series. For both cyclic and fan TiC_n^+ clusters doublet ground states were generally obtained. In the case of linear and cyclic TiC_n^- clusters we found that quartet ground states are favored over doublet ones. Finally in fan TiC_n^- structures we found doublet states more stable than quartet ones with the only exception of TiC_8^- where both states are practically isoenergetic.

Concerning geometrical data, we conclude that fan $TiC_n^{+/-}$ present larger Ti–C bond distances than cyclic and linear structures. In general we have observed the same pattern in the C–C bond distances, C_{odd}–C_{even} distances shorter than C_{even}–C_{odd}.

We have computed the incremental binding energies for the different clusters studied in order to discus their relative stability. For linear and fan cationic clusters an odd–even alternation in stability was found, *n*-even clusters were more stable than those with *n*-odd. In linear and fan anionic isomers, a clear even–odd alternation in stability was observed; *n*-even clusters were more stables than the adjacent *n*-odd ones. However as the number of carbon atoms increases the incremental binding energy converges to an almost constant value. For cyclic cationic and anionic clusters, we could not found a general pattern in the incremental binding energies because the lack of data.

Concerning the competition between linear, fan and cyclic structures, our study suggests that for small clusters the lowest-lying states correspond to fan type isomers and cyclic structures are favored for largest ones.

In addition we have computed ionization potentials and adiabatic electron affinities for linear, cyclic and fan TiC_n clusters. Ionization potentials show a parity alternation effect especially for the fan conformations: systems with an odd number of carbon atoms present higher ionization potentials than the adjacent with an even number of carbons. In the electron affinities we observe also a clear alternation effect especially for the linear structures, with *n*-even clusters having higher values.

Acknowledgements

This research has been supported by the Ministerio de Educación y Ciencia of Spain (Grant CTQ2004-07405-C02-01) and by the Junta de Castilla y León (Grant VA 077A06).

Appendix A. Supplementary data

Supplementary data associated with this article can be found, in the online version, at doi:10.1016/j.ijms.2007.06.023.

References

[1] W. Weltner Jr., R.J. Van Zee, Chem. Rev. 89 (1989) 1713.
[2] K. Raghavachari, J.S. Binkley, J. Chem. Phys. 87 (1987) 2191.
[3] A. Van Orden, R.J. Saykally, Chem. Rev. 98 (1998) 2313.
[4] K.H. Hinkle, J.J. Keady, P.F. Bernath, Science 241 (1988) 1319.
[5] P.F. Bernath, K.H. Hinkle, J.J. Keady, Science 244 (1989) 562.
[6] A.E. Douglas, Astrophys. J. 114 (1951) 466.
[7] L.M. Haffner, D.M. Meyer, Astrophys. J. 433 (1995) 450.
[8] D.E. Woon, E. Herbst, Astrophys. J. 465 (1996) 795.
[9] R.P.A. Bettens, E. Herbst, Astrophys. J. 468 (1996) 686.
[10] R.P.A. Bettens, E. Herbst, Astrophys. J. 478 (1997) 585.
[11] J. Fulara, D. Lessen, P. Freivogel, J.P. Maier, Nature 366 (1993) 439.
[12] P. Freivogel, J. Fulara, J.P. Maier, Astrophys. J. 431 (1994) L151.
[13] H. Koinuma, T. Horiuchi, K. Inomata, H.-K. Ha, K. Nakajina, K.A. Chaudhary, Pure Appl. Chem. 68 (1996) 1151.
[14] M.D. Allendorf, J. Electrochem. Soc. 140 (1993) 747.
[15] K.S. Pitzer, E. Clementi, J. Am. Chem. Soc. 81 (1959) 4477.
[16] M. Leleyter, P. Joyes, Surf. Sci. 156 (1985) 800.
[17] O. Matsumoto, T. Kotaki, H. Shikano, K. Takemura, S. Tanaka, J. Electrochem. Soc. 141 (1994) L16.
[18] P. Botschwina, M. Horn, K. Markey, R. Oswald, Mol. Phys. 92 (1997) 381.
[19] J.C. Rienstra-Kiracofe, B.G. Ellison, B.C. Hoffman, H.F. Schaefer, J. Phys. Chem. A 104 (2000) 2273.
[20] F. Pauzat, Y. Ellinger, Astron. Astrophys. 216 (1989) 305.
[21] M.C. MacCarthy, M.J. Travers, P. Kalmus, C.A. Gottlieb, P. Thaddeus, Astrophys. J. 467 (1996) L125.
[22] J. Cernicharo, M. Guelin, Astron. Astrophys. 309 (1996) L27.
[23] M. Guelin, J. Cernicharo, M.J. Travers, M.C. MacCarthy, C.A. Gottlieb, P. Thaddeus, M. Ohishi, S. Saito, S. Yamamoto, Astron. Astrophys. 317 (1997) L1.
[24] G. Schermann, T. Grösser, F. Hampel, A. Hirsch, Chem. Eur. J. 3 (1997) 1105.
[25] R. Dembinski, T. Bartik, B. Bartik, M. Jaeger, J.A. Gladysz, J. Am. Chem. Soc. 122 (2000) 810.
[26] M.J. Leleyter, Phys. II 1 (1991) 1179.
[27] M. Leleyter, Z. Phys. D 12 (1989) 381.
[28] M. Leleyter, Z. Phys. D 20 (1991) 81.
[29] M. Leleyter, Z. Phys. D 20 (1991) 85.
[30] C.R. Wang, R.B. Huang, Z.Y. Liu, L.S. Zheng, Chem. Phys. Lett. 227 (1994) 103.
[31] C.R. Wang, R.B. Huang, Z.Y. Liu, L.S. Zheng, Chem. Phys. Lett. 237 (1995) 463.
[32] Z.Y. Liu, R.B. Huang, Z.C. Tang, L.S. Zheng, Chem. Phys. 229 (1998) 335.
[33] C.R. Wang, R.B. Huang, Z.Y. Liu, L.S. Zheng, Chem. Phys. Lett. 227 (1994) 109.
[34] C.G. Zhan, S.J. Iwata, Chem. Phys. 104 (1996) 9058.
[35] C.G. Zhan, S.J. Iwata, J. Chem. Phys. 105 (1996) 6578.
[36] C.G. Zhan, S.J. Iwata, Phys. Chem. A 101 (1997) 591.
[37] C.G. Zhan, S.J. Iwata, Chem. Phys. 107 (1997) 7323.
[38] G. Pascoli, H. Lavendy, Chem. Phys. Lett. 312 (1999) 333.
[39] G. Pascoli, H. Lavendy, J. Phys. Chem. A 103 (1999) 3518.
[40] K. Fisher, I. Dance, G. Willett, Eur. Mass Spectrom. 3 (1997) 331.
[41] G.L. Li, Z.C. Tang, J. Phys. Chem. A 107 (2003) 5317.
[42] A. Largo, P. Redondo, C. Barrientos, J. Phys. Chem. A 106 (2002) 4217.
[43] P. Redondo, C. Barrientos, A. Cimas, A. Largo, J. Phys. Chem. A 107 (2003) 4676.
[44] P. Redondo, C. Barrientos, A. Cimas, A. Largo, J. Phys. Chem. A 107 (2003) 6317.
[45] A. Largo, P. Redondo, C. Barrientos, J. Phys. Chem. A 108 (2004) 6421.
[46] P. Redondo, C. Barrientos, A. Largo, Int. J. Quantum Chem. 96 (2004) 615.
[47] S. Hunsicker, R.O. Jones, J. Chem. Phys. 105 (1996) 5048.
[48] M. Gomei, R. Kishi, A. Nakajima, S. Iwata, K. Kaya, J. Chem. Phys. 107 (1996) 10051.
[49] H.Y. Wang, R.B. Huang, H. Chen, M.H. Lin, L.S. Zheng, J. Phys. Chem. A 105 (2001) 4653.
[50] R. Vandenbosch, D.I. Will, J. Chem. Phys. 104 (1996) 5600.
[51] L. Pan, B.K. Rao, A.K. Gupta, G.P. Das, P. Ayyub, J. Chem. Phys. 119 (2003) 7705.
[52] H.J. Zhai, L.S. Wang, P. Jena, G.L. Gutsev, C.W. Bauschlicher Jr., J. Chem. Phys. 120 (2004) 8996.
[53] D.L. Strout, M.B. Hall, J. Phys. Chem. 100 (1996) 18007.
[54] S. Roszak, K. Balasubramanian, J. Chem. Phys. 106 (1997) 158.
[55] D.L. Strout, M.B. Hall, J. Phys. Chem. A 102 (1998) 641.
[56] D.G. Dai, S. Roszak, K. Balasubramanian, J. Phys. Chem. A 104 (2000) 9760.
[57] D.L. Strout, T.F. Miller III, M.B. Hall, J. Phys. Chem. A 102 (1998) 6307.
[58] T.F. Miller III, M.B. Hall, J. Am. Chem. Soc. 121 (1999) 7389.
[59] P. Redondo, C. Barrientos, A. Largo, J. Phys. Chem. A 109 (2005) 8594.
[60] P. Redondo, C. Barrientos, A. Largo, J. Phys. Chem. A 110 (2006) 4057.
[61] P. Redondo, C. Barrientos, A. Largo, J. Chem. Theory Comput. 2 (2006) 885.
[62] P. Redondo, C. Barrientos, A. Largo, J. Mol. Struct. (Theochem.) 769 (2006) 225.
[63] H.C. Urey, Phys. Rev. 88 (1952) 248.
[64] A. Fowler, Mont. Not. Roy. Astron. Soc. 69 (1909) 508.
[65] T.J. Bernatowicz, O.W. Akande, T. Croat, R. Cowsik, Astrophys. J. 631 (2005) 988.
[66] B.C. Guo, K.P. Kerns, A.W. Castleman, Science 255 (1992) 1411.
[67] B.C. Guo, S. Wei, J. Purnell, S. Buzza, A.W. Castleman, Science 256 (1992) 515.
[68] J.S. Pilgrim, M.A. Duncan, J. Am. Chem. Soc. 115 (1993) 6958.
[69] B.V. Reddy, S.N. Khanna, Chem. Phys. Lett. 209 (1993) 104.
[70] B.V. Reddy, S.N. Khanna, J. Phys. Chem. 988 (1994) 9446.
[71] S. Wei, B.C. Guo, J. Purnell, S. Buzza, A.W. Castleman, J. Phys. Chem. 96 (1992) 4166.
[72] S.F. Cartier, B.D. May, A.W. Castleman, J. Phys. Chem. 100 (1996) 8175.
[73] J.S. Pilgrim, L.R. Brock, M.A. Duncan, J. Phys. Chem. 99 (1995) 544.
[74] L.R. Brock, M.A. Duncam, J. Phys. Chem. 100 (1996) 5654.
[75] C.S. Yeh, Y.G. Byun, S. Afzaal, S.Z. Kan, S.A. Lee, B.S. Freiser, P.J. Hay, J. Am. Chem. Soc. 117 (1995) 4042.
[76] Y.G. Byun, S.Z. Kan, S.A. Lee, Y.H. Kim, M. Miletic, R.E. Bleil, S. Kais, B.S. Freiser, J. Phys. Chem. 100 (1996) 6336.
[77] S. Lee, N.G. Gotts, G. von Helden, M.T. Bowers, Science 267 (1995) 999.
[78] M.D. Hack, R.G.A.R. Maclagan, G.E. Scuseria, M.S. Gordon, J. Chem. Phys. 104 (1996) 6628.
[79] A. Kalemos, A. Mavridis, J. Phys. Chem. A 106 (2002) 3905.
[80] C.W. Bauschlicher, Theor. Chem. Acc. 110 (2003) 153.
[81] R. Sumathi, M. Hendrickx, Chem. Phys. Lett. 287 (1998) 496.
[82] R. Sumathi, M. Hendrickx, J. Phys. Chem. A 102 (1998) 4883.
[83] A.D. Becke, J. Chem. Phys. 98 (1993) 5648.
[84] I.S.K. Kerkines, A. Mavridis, J. Phys. Chem. A 104 (2000) 11777.

[85] X.B. Wang, C.F. Ding, L.S. Wang, J. Phys. Chem. A 101 (1997) 7699.
[86] L. Largo, A. Cimas, V.M. Rayón, C. Barrientos, Chem. Phys. 330 (2006) 431.
[87] R. Krishnan, J.S. Binkley, R. Seeger, J.A. Pople, J. Chem. Phys. 72 (1980) 650.
[88] A.J.H. Wachters, J. Chem. Phys. 52 (1970) 1033.
[89] P.J. Hay, J. Chem. Phys. 66 (1977) 4377.
[90] K. Raghavachari, G.W. Trucks, J. Chem. Phys. 91 (1989) 1062.
[91] P.J. Stephens, F.J. Devlin, C.F. Chabalowski, M.J. Frisch, J. Phys. Chem. 98 (1994) 11623.
[92] C. Lee, W. Yang, R.G. Parr, Phys. Rev. B 37 (1988) 785.
[93] A.D. Becke, J. Chem. Phys. 88 (1988) 1053.
[94] G. Pascoli, H. Lavendy, Int. J. Mass Spectrom. 181 (1998) 11.
[95] M.J. Frisch, G.M. Trucks, H.B. Schlegel, G.E. Scuseria, M.A. Robb, J.R. Cheeseman, V.G. Zakrzewski, J.A. Montgomery Jr., R.E. Stratmann, J.C. Burant, S. Dapprich, J.M. Millan, A.D. Daniels, K.N. Kudin, M.C. Strain, O. Farkas, J. Tomasi, V. Barone, M. Cossi, R. Cammi, B. Mennucci, C. Pomelly, C. Adamo, S. Clifford, J. Ochterski, G.A. Petersson, P.Y. Ayala, Q. Cui, K. Morokuma, D.K. Malick, A.D. Rabuck, K. Raghavachari, J.B. Foresman, J. Cioslowski, J.V. Ortiz, A.G. Baboul, B.B. Stefanov, G. Liu, A. Liashenko, P. Piskorz, I. Komaromi, R. Gomperts, R.L. Martin, D.J. Fox, T. Keith, M.A. Al-Laham, C.Y. Peng, A. Nanayakkara, C. Gonzalez, M. Challacombe, P.M.W. Gill, B. Johnson, W. Chen, M.W. Wong, J.L. Andres, C. Gonzalez, M. Head-Gordon, E.S. Replogle, J.A. Pople, Gaussian 98, Gaussian Inc., Pittsburgh, PA, 1998.
[96] D.E. Clemmer, J.L. Elkind, N. Aristov, P.B. Armentrout, J. Chem. Phys. 95 (1991) 3387.
[97] G.L. Gutsev, L. Andrews, C.W. Bauschlicher, Theor. Chem. Acc. 109 (2003) 298.